

# Fuzzy-Tuning Current-Vector Control of a Three-Phase PWM Inverter for High-Performance AC Drives

Ying-Yu Tzou, *Member, IEEE*, and Shiu-Yung Lin

**Abstract**— This paper proposes a new discrete fuzzy-tuning current-vector control (FTC) scheme for three-phase pulsewidth modulation (PWM) inverters. The proposed current control scheme can achieve fast transient responses and, at the same time, have very low total harmonic distortion in output current during steady-state operation. The proposed FTC scheme generates quasi-optimum PWM patterns by using a closed-loop control technique with instantaneous current feedback. The proposed FTC scheme has been realized using a single-chip digital signal processor (TMS320C14) from Texas Instruments. Experimental results are given to verify the proposed fuzzy-tuning current control strategy for three-phase PWM inverters.

**Index Terms**— Current vector control, digital signal processor, fuzzy control, pulsewidth modulation inverter.

## I. INTRODUCTION

A CURRENT control loop is usually employed in a high-performance electrical drive to achieve fast torque control. In adjustable-speed ac drives, the pulsewidth modulation (PWM) voltage control is usually associated with the stator current control, because the current is directly related to the motor developed torque. The current control strategy plays a most important role in a vector-controlled ac drive, in which the quick current responses and low harmonic current content to suppress torque ripples and phonic noises are required. The employment of voltage-source current-controlled PWM inverters (VCI's) in high-performance ac servo drives has the following advantages [1], [2].

- The bulky and noisy choke used in a current-source inverter can be eliminated.
- The VCI can be used in a multiple drive system with common dc link, while this is not possible for the current-source inverter.
- The VCI can achieve better regulated sinusoidal current waveform with controlled harmonics and has an inherent short-circuit protection and peak current suppression capability.
- Dynamic braking is simple for a VCI drive, which allows fast-response four-quadrant operation.

Manuscript received December 4, 1995; revised March 30, 1998. Abstract published on the Internet July 3, 1998. This work was supported by the National Science Council, Taipei, Taiwan, R.O.C., under Project NSC 86-2213-E-009-042.

The authors are with the Department of Electrical and Control Engineering, National Chiao Tung University, Hsinchu, 30050 Taiwan, R.O.C. (e-mail: yytzou@cc.nctu.edu.tw; u8612801@cc.nctu.edu.tw).

Publisher Item Identifier S 0278-0046(98)07026-9.

A variety of current control schemes has been investigated and reported for the closed-loop current regulation of three-phase PWM inverters [3], [4]. Among the current control techniques, hysteresis current control is the simplest and most extensively used method [5], [6]. Besides the fast response and the inherent current-limiting capability, this technique does not require any load information. Nevertheless, a current controller with fixed hysteresis band has major disadvantages of varying switching frequency and larger current ripples and, theoretically, it can reach double the value of the hysteresis bands [7]. As a result, the load current contains harmonics that cause additional machine heating. An adaptive hysteresis band current controller can maintain the switching frequency constant or within a specified range [8], [9]. However, techniques available to overcome these limitations are complex to implement and require extensive knowledge of the system parameters.

Conventional current controllers for ac motor drives usually regulate the three-phase currents independently and are usually realized using an analog circuit. However, the analog circuit, which is required to realize the coordinate transformation, current control law, and PWM signal generation, is complex to realize. Furthermore, it also suffers from demerits of the analog circuit, such as offset drifting, aging effect, and low noise immunity. Software current control techniques, on the other hand, provide a more flexible approach in the realization of current control schemes for three-phase PWM inverters. However, the limited sampling rate and finite word length of the microprocessor will also impose a limitation on the current loop bandwidth.

Space-vector PWM (SVPWM) technique has been proposed to generate a PWM gating signal with optimal flux trajectory, but, since there are inevitable parameter variations in the ac motor and PWM inverter drive, current ripple and flux ripple still occur. Therefore, closed-loop control of the motor phase currents is still required to minimize this effect and, at the same time, to achieve fast current response. In recent years, the SVPWM technique has been widely adopted in the inverter drive for the open-loop speed control of three-phase ac motors [10]–[12]. The concept of space-vector control was then extended to the closed-loop current vector control of three-phase inverter drives [13], [14].

Habetler and Divan [15] proposed a space-vector-based hysteresis current controller. However, the current ripples in steady-state responses are still large. An SVPWM-based

three-level hysteresis technique was presented in [16]; it adds zero-voltage vectors in the hysteresis current controller to improve steady-state performance, while the width of the middle level cannot be defined as a function of steady-state performance. Deadbeat control in two-phase current plane to control motor current can achieve good dynamic responses, but it is very sensitive to parameter variations [17]. Current control with prediction action has also been proposed to improve the steady-state performance of an inverter drive, but it has the drawback of needing accurate information of the motor speed and parameters [18].

Fuzzy control technique was also employed in the current regulation of three-phase PWM inverters [19]. However, the proposed method was applied to the independent control of three-phase currents and the fuzzy control laws were also just based on the phase current error and its derivatives. This paper proposes a new space-vector-based fuzzy-tuning current control scheme for three-phase PWM inverters. A heuristic fuzzy-tuning algorithm was developed to adjust the current-vector control gains such that the generated PWM patterns can result in a circular current-vector trajectory with minimum current ripple in steady state. The fuzzy-tuning current-vector control (FTC) scheme uses only instantaneous phase current as feedback signals and without knowing any other system parameters. The operating principle and fuzzy-tuning strategy of the proposed current control scheme are described in detail in this paper.

## II. DISCRETE CURRENT CONTROL SCHEME

Fig. 1 shows the schematic of a three-phase voltage-source PWM inverter connected with a steady-state equivalent circuit of a balanced Y-connected three-phase ac motor. The fundamental components of the motor phase currents are shown in Fig. 2(a). In the complex plane perpendicular to the motor axis, as shown in Fig. 2(b), a stator current vector can be formed by combining the instantaneous three-phase quantities

$$\mathbf{i}_s = i_{as} + i_{bs}e^{j(2\pi/3)} + i_{cs}e^{j(4\pi/3)} = i_\alpha + j i_\beta. \quad (1)$$

This current vector can also be represented in a matrix form as

$$\mathbf{i}_s = \begin{bmatrix} i_\alpha \\ i_\beta \end{bmatrix} = \begin{bmatrix} 1 & 0 & 0 \\ 0 & -\frac{1}{\sqrt{3}} & \frac{1}{\sqrt{3}} \end{bmatrix} \begin{bmatrix} i_{as} \\ i_{bs} \\ i_{cs} \end{bmatrix} = \mathbf{C} \begin{bmatrix} i_{as} \\ i_{bs} \\ i_{cs} \end{bmatrix} \quad (2)$$

where  $\mathbf{C}$  is the Clarke transformation matrix. The voltage vector  $\mathbf{v}_s$  and the back-EMF voltage vector  $\mathbf{e}$  of the three-phase circuit can also be expressed in the same way. These vector quantities have the following relationship:

$$\mathbf{v}_s(t) = \mathbf{i}_s(t)R_s + L_s \frac{d\mathbf{i}_s(t)}{dt} + \mathbf{e}(t). \quad (3)$$

For the current controller used in a motor drive, it is desired to track a given reference current command with minimum tracking error in transient response and minimum current ripple during steady-state response. In conventional voltage-source current-controlled PWM inverters, the motor phase currents are controlled by three independently hysteresis-controlled current regulators. However, such current control

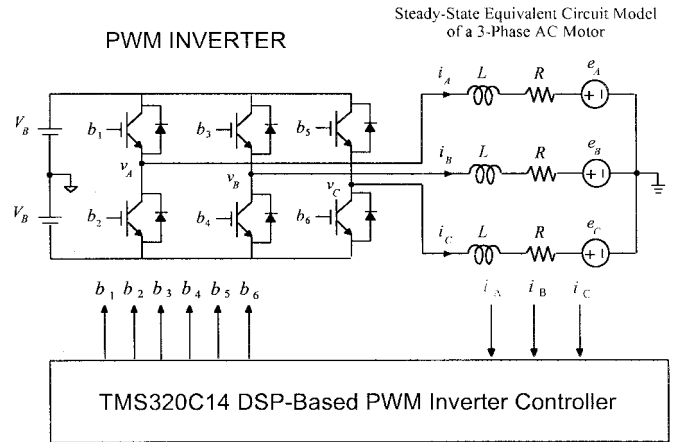
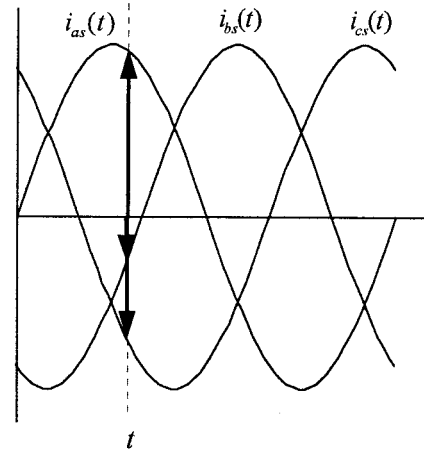
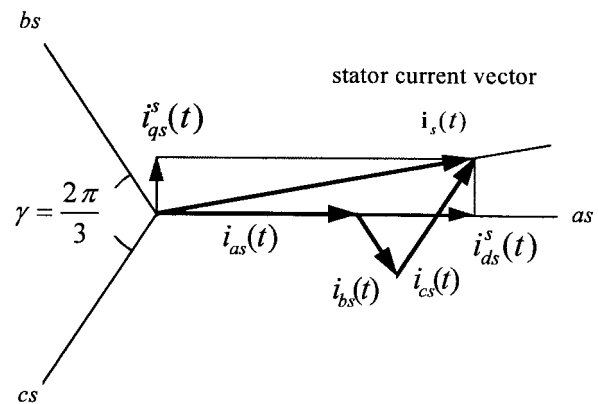


Fig. 1. A three-phase voltage-source digital-signal-processor (DSP)-controlled PWM inverter with equivalent circuit of a balanced three-phase load.



(a)



(b)

Fig. 2. (a) Balanced three-phase current. (b) Current-vector representation in stationary  $\alpha$ - $\beta$  coordinates.

schemes cannot ensure a minimum current ripple in the current vector. The performance of a field-oriented vector-controlled ac drive depends on two major factors. One is the current loop bandwidth, and the other is the effectiveness

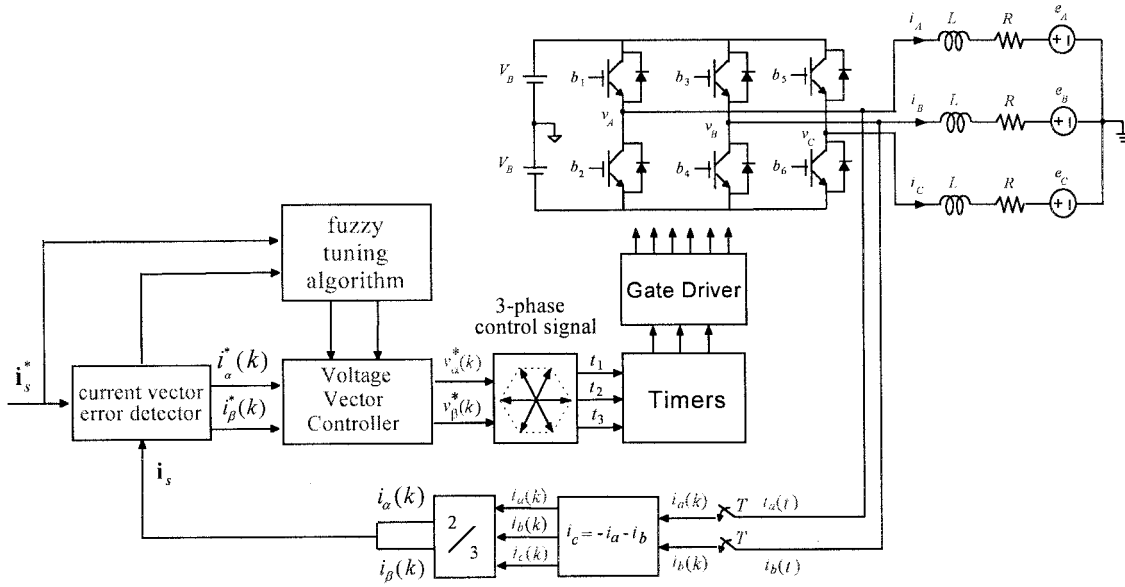


Fig. 3. System block diagram of the proposed self-tuning current-controlled PWM inverter controller.

of the decoupling control. Conventionally, the current-loop controller is realized using analog techniques to achieve a high bandwidth. However, with the great advances in high-performance DSP's, now it is possible to realize more flexible current control strategies using software control techniques. Fig. 3 shows the system block diagram of the proposed FTC controller. The purpose of the current controller is to make the current trajectory follow a set of reference current waveforms by using eight voltage vectors switched by the three-phase voltage-source inverter.

From (3), we can see that the stator current is a function of the applied stator voltage and resultant motor back EMF; it also depends upon the stator winding resistance and inductance. The solution of (3) is

$$\mathbf{i}_s(t) = \frac{\mathbf{v}_s(t) - \mathbf{e}(t)}{R_s} - \left[ \frac{\mathbf{v}_s(t) - \mathbf{e}(t)}{R_s} - \mathbf{i}_s(t_0) \right] e^{-(R_s/L_s)t} \quad (4)$$

where  $\mathbf{i}_s(t_0)$  is the initial current. The back-EMF voltage vector  $\mathbf{e}(t)$  can be considered constant over a sampling interval for the digital control. At  $t = t_0 + T$ , this current vector can be expressed as

$$\mathbf{i}_s(t_0 + T) = \frac{\mathbf{v}_s(t_0 + T) - \mathbf{e}(t_0 + T)}{R_s} - \left[ \frac{\mathbf{v}_s(t_0 + T) - \mathbf{e}(t_0 + T)}{R_s} - \mathbf{i}_s(t_0) \right] \cdot e^{-(R_s/L_s)(t_0 + T)} \quad (5)$$

where  $T$  is the sampling period of the current controller. Equation (5) can be expressed in its discrete form to get a simple notation

$$\mathbf{i}_s(k+1) = \Delta \mathbf{i}_e(k+1) - [\Delta \mathbf{i}_e(k+1) - \mathbf{i}_s(k)] e^{-(T/\tau_s)} \quad (6)$$

where  $\tau_s$  is the electrical time constant of the stator winding and

$$\Delta \mathbf{i}_e(k+1) = \frac{\mathbf{v}_s(k+1) - \mathbf{e}(k+1)}{R_s} \quad (7)$$

is the effective current correction vector. Equation (6) can be further reduced to

$$\Delta \mathbf{i}_e(k+1) = \mathbf{i}_s(k+1) \frac{1}{\lambda} - \mathbf{i}_s(k) \quad (8)$$

where  $\lambda = \exp(-T/\tau_s)$ . If we let  $\mathbf{i}_s(k+1)$  be the desired current command  $\mathbf{i}_s^*(k)$ , then the current correction vector in the  $k$ th sampling interval is

$$\Delta \mathbf{i}_e(k) = \mathbf{i}_s^*(k) \frac{1}{\lambda} - \mathbf{i}_s(k) \quad (9)$$

and the corresponding voltage vector is

$$\mathbf{v}_s(k) = \Delta \mathbf{i}_e(k) R_s + \mathbf{e}(k). \quad (10)$$

This implies that, if the resistance and inductance of the stator winding are known and the motor back EMF is also known, then a voltage correction vector can be synthesized to achieve deadbeat current control effect. However, these conditions are hard to meet in practical situations due to parameter variations and unknown back EMF. Although the back EMF can be estimated from the speed feedback, it should be noted that this is also based on a well-tuned motor drive. Furthermore, for the PWM inverter drives or sensorless drives, there is no available speed feedback. Therefore, it is desired to design an autotuning current controller so that fast response and minimum current ripple in vector space can be achieved.

Fig. 4 shows the desired current vector  $\mathbf{i}_s^*(k)$  and the measured feedback current vector  $\mathbf{i}_s(k)$ . The purpose of the current controller is to synthesize a voltage correction vector so

that the current error vector  $\Delta \mathbf{i}_s(k)$  can be kept to a minimum value. The error current vector is defined as

$$\Delta \mathbf{i}_s(k) = \mathbf{i}_s^*(k) - \mathbf{i}_s(k) \quad (11)$$

where  $\mathbf{i}_s^*(k)$  is the specified current-vector command and  $\mathbf{i}_s(k)$  is the measured current-vector feedback. Combining with (10), the current correction vector can be expressed as

$$\Delta \mathbf{i}_c(k) = \frac{1}{\lambda} [\mathbf{i}_s(k)(1 - \lambda) + \Delta \mathbf{i}_s(k)]. \quad (12)$$

A discrete proportional integral (PI) controller is used to generate the required voltage vector according to this current correction vector. The discrete PI current loop controller has the form

$$\mathbf{v}_s(k) = \left[ K_p + \frac{K_i}{1 - z^{-1}} \right] \Delta \mathbf{i}_c(k) \quad (13)$$

and the velocity form or incremental form of this PI control algorithm can be derived as

$$\mathbf{v}_s(k) = \mathbf{v}_s(k-1) + K_p[\Delta \mathbf{i}_c(k) - \Delta \mathbf{i}_c(k-1)] + K_i \Delta \mathbf{i}_c(k). \quad (14)$$

This stator voltage vector is composed of two orthogonal vectors  $v_\alpha$  and  $v_\beta$  which are derived from their corresponding current components in  $\alpha$ - $\beta$  coordinates

$$v_\alpha(k) = v_\alpha(k-1) + K_p[\Delta i_{e\alpha}(k) - \Delta i_{e\alpha}(k-1)] + K_i \Delta i_{e\alpha}(k), \quad (15)$$

$$v_\beta(k) = v_\beta(k-1) + K_p[\Delta i_{e\beta}(k) - \Delta i_{e\beta}(k-1)] + K_i \Delta i_{e\beta}(k). \quad (16)$$

A fuzzy-tuning algorithm is developed to adjust the control gains such that the motor current vector will follow the command current vector with minimum current ripple. Fig. 5 shows the block diagram of the proposed FTC controller. The gains of the PI controller are tuned by the following rules:

$$\begin{aligned} K_p(k) &= K_p(k-1) + \Delta K_p \\ K_i(k) &= K_i(k-1) + \Delta K_i \end{aligned} \quad (17)$$

and the tuning incremental  $\Delta K_p$  and  $\Delta K_i$  are determined by a rule-based fuzzy-tuning algorithm. The stator voltage vectors determined by (15) and (16) are then transformed to the control duty ratios for the PWM inverter

$$\begin{bmatrix} d_a(k) \\ d_b(k) \\ d_c(k) \end{bmatrix} = \frac{2}{V_{dc}} \begin{bmatrix} 1 & 0 \\ -0.5 & -\sqrt{3}/2 \\ -0.5 & \sqrt{3}/2 \end{bmatrix} \begin{bmatrix} v_\alpha(k) \\ v_\beta(k) \end{bmatrix}. \quad (18)$$

These PWM gating signals can be generated by the programmable timers of a microprocessor. However, it should be noted that the corresponding output gating signals should be *encased* and *symmetric*, as shown in Fig. 6, to keep low harmonics during steady state.

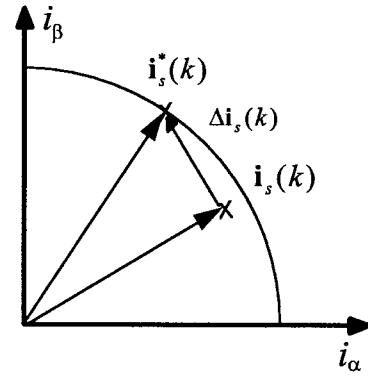


Fig. 4. Desired current trajectory.

### III. FUZZY-TUNING CURRENT CONTROL SCHEME

Fuzzy set theory first introduced by Zadeh [20] was used to describe inexact information. Most early research work on fuzzy theory was carried out in the field of mathematics and social science. However, after Mamdani's pioneer work on its application to the control of a steam engine [21], many applications of fuzzy control in industrial applications were developed [22]. The most significant feature of fuzzy logic control (FLC) is that it provides a systematic approach to convert linguistic control strategy based on expert experience and knowledge to an automatic control strategy [23], [24]. The fuzzy control algorithm consists of a set of linguistic rules related by the concepts of fuzzy implication, approximate reasoning, and compositional rule of inference. The linguistic rules are usually derived from expert experience or constructed through an empirical learning process [25]–[27]. Because the detailed dynamics of the controlled process is not needed in the design process, fuzzy control possesses an inherent robustness [28], [29].

The inputs to the fuzzy-tuning controller are the averaged amplitude of the current command vector and the summation of squares of current error vector. The averaged amplitude of the current command vector is calculated by

$$\bar{\mathbf{I}}_s(k) = \bar{\mathbf{I}}_s(k-1) + \mathbf{i}_s(k) \frac{1}{N} (1 - z^{-N}) \quad (19)$$

and the summation of squares of current error vector is

$$\Delta \mathbf{I}_s(k) = \Delta \mathbf{I}_s(k-1) + \Delta \mathbf{i}_s^2(k) \frac{1}{N} (1 - z^{-N}) \quad (20)$$

where  $N$  is the number of samples in one iteration cycle of the stator current-vector command.

In the design of a fuzzy controller, one should first identify the feedback (input) and control (output) variables and determine a term set which is at a suitable level of granularity for describing the values of each linguistic variable. The proposed FTC controller uses (19) and (20) as the input linguistic variables, and the incremental changes  $\Delta K_p$  and  $\Delta K_i$  for the PI controller are chosen as output linguistic variables.

There is no particular theory to justify how many terms (fuzzy subsets) are best in describing a linguistic variable. However, increasing the terms will also result in increasing the rules, and this further complicates the rule generation.

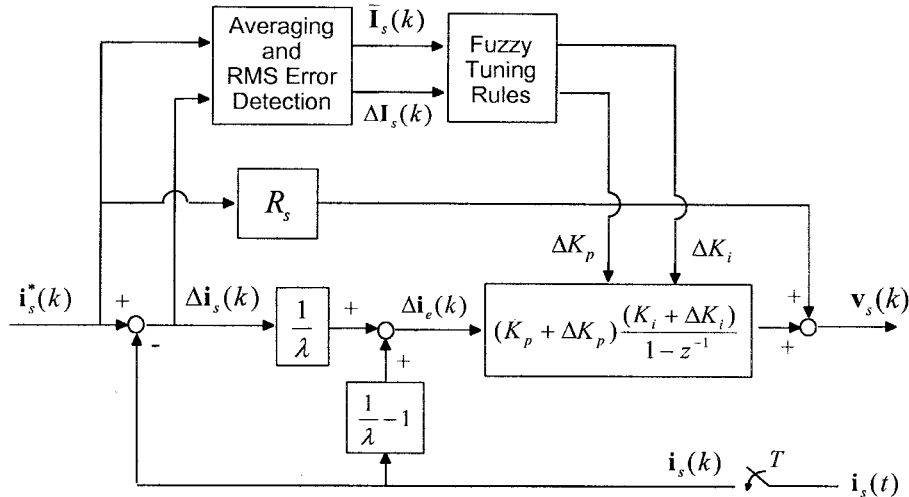


Fig. 5. Block diagram of the FTC controller.

The number of fuzzy quantifiers also depends on the semantic interpretation of physical quantity. In the proposed FTC, a five-term set {large positive (LP), medium positive (MP), zero (ZE), medium negative (MN), large negative (LN)} was used to define each linguistic variable.

The determination of the membership functions quite depends on the designer's experiences and experts' knowledge. It is not so trivial to choose a particular shape that is better than others. Triangle, trapezoid, and bell shape are the three most popular candidates in most applications. The triangle-shaped membership function has the advantages of simplicity and easier implementation and is chosen in this application. Fig. 7 shows the membership functions of the input and output linguistic variables.

In the design of a fuzzy control system, the formulation of its rule set plays a key role in the improvement of system performance. These fuzzy rules are a set of {IF ..., THEN ...} statements. A typical example is defined as

IF command is LP and error is LP, THEN control is LP.

This means that, if the command is large positive (LP) and the error is also large positive (LP), then the control output should be large positive (LP). In the proposed fuzzy-tuning controller, we developed 13 fuzzy tuning rules for each output variable and, because of the symmetric property of the fuzzy variables, there were 25 rules in total for each output variable. For example, the fuzzy tuning rules for the proportional gain are a set of {IF ..., THEN ...} statements

- $R_1$ : IF  $\bar{I}_s(k)$  is LP and  $\Delta I_s(k)$  is LN, THEN  $\Delta K_p$  is LP,  
 $R_2$ : IF  $\bar{I}_s(k)$  is LP and  $\Delta I_s(k)$  is MN, THEN  $\Delta K_p$  is MP,  
 ...,  
 $R_{25}$ : IF  $\bar{I}_s(k)$  is LN and  $\Delta I_s(k)$  is LP, THEN  $\Delta K_p$  is LN.

These rules can be tabulated as shown in Fig. 7(e) and (f) for easy reference. In the developed tuning algorithm, the command current vector has a major influence on the tuning of the proportional gain, while the summation of error squares

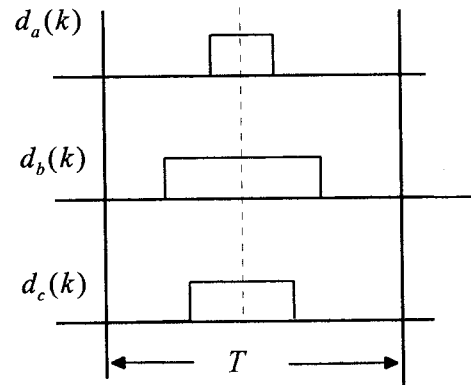


Fig. 6. PWM gating signals to the three-phase inverter.

has a major influence on the tuning of integral gain. One reason that explains the inherent robustness characteristics of fuzzy control is that its control action is determined by the compositional inference from a set of rules. These rules were generally developed based on practical experiences or heuristic analysis and without knowing the detailed mathematical model and parameters of the plant. Various inference mechanisms have been developed to defuzzify the fuzzy rules [30]. The two methods most frequently used in fuzzy reasoning are the max-min and max-dot inference methods. In this paper, we applied the max-min inference method to get the implied fuzzy set of the tuning action from a set of fuzzy tuning rules.

The imprecise fuzzy control action generated from the inference engine must be transformed to a precise control action in real applications. The center-of-mass method was used to defuzzify the implied fuzzy control variables. The developed fuzzy tuning process can be realized by prescanning a specified range of input fuzzy variables and then tabulating the corresponding input and output variables. This calculated fuzzy decision table can be stored in an erasable programmable read-only memory (EPROM) and can be referenced either using software or hardware techniques.

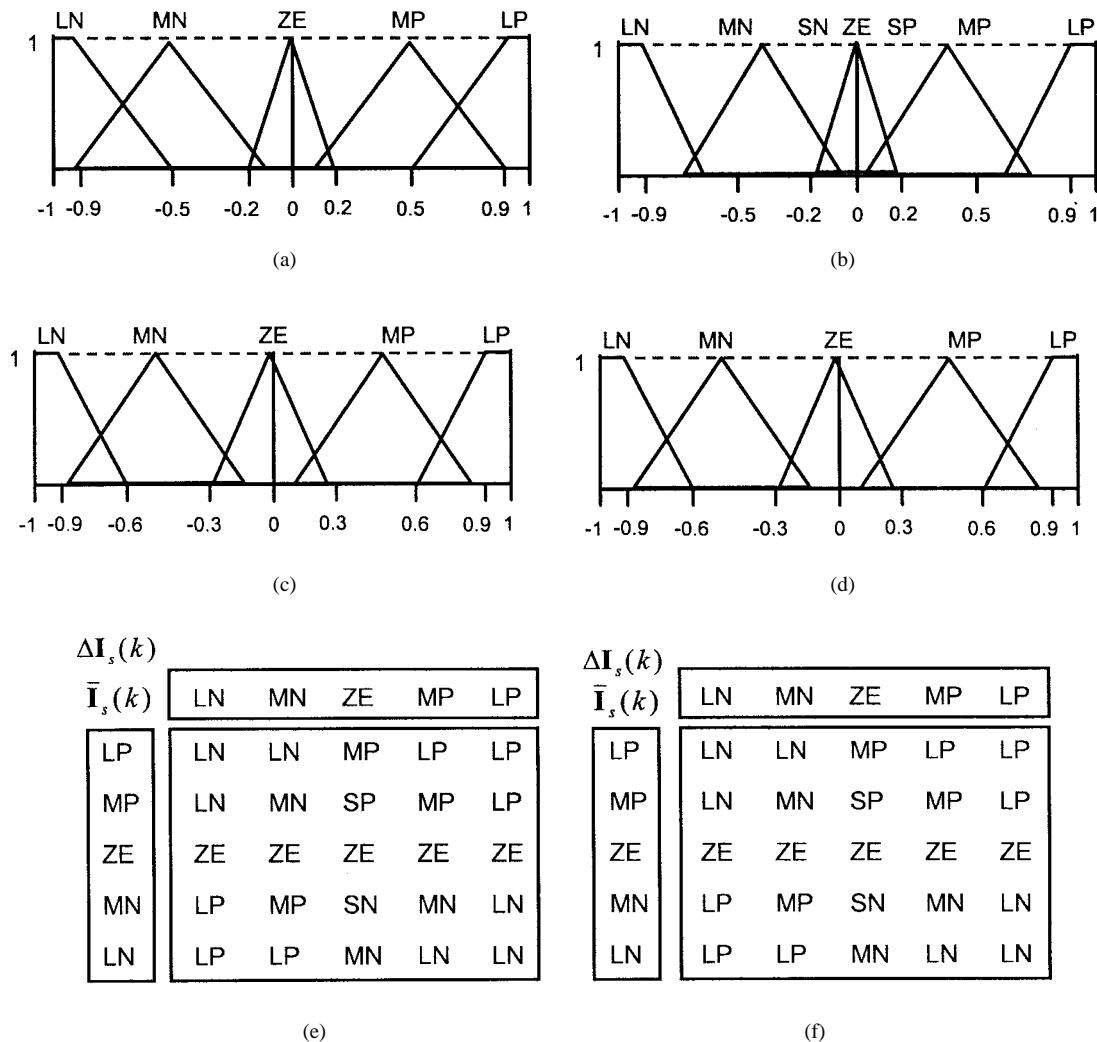


Fig. 7. Membership function of the (a) current command  $\bar{I}_s(k)$ , (b) current error  $\Delta I_s(k)$ , (c) increment for proportional gain  $\Delta K_p$ , (d) increment for integral gain  $\Delta K_i$ , and rule tables for the fuzzy tuning of the (e) proportional  $\Delta K_p$  and (f) integral gains  $\Delta K_i$ .

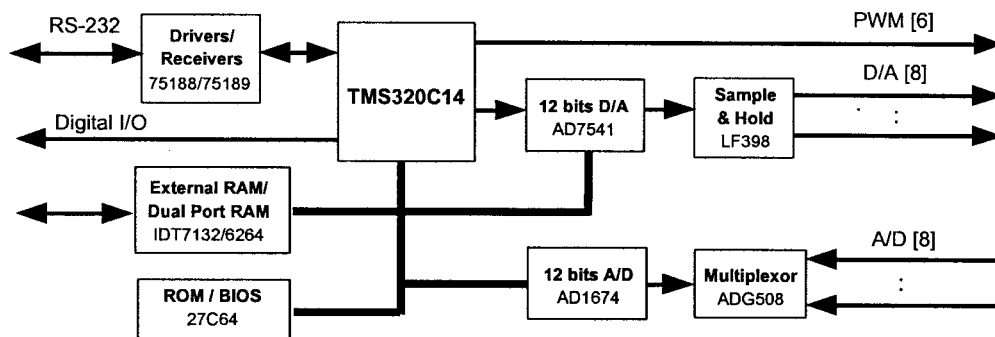


Fig. 8. Block diagram of the single-chip DSP-based digital control board.

#### IV. IMPLEMENTATION AND EXPERIMENTAL RESULTS

There are various approaches to the realization of a fuzzy controller [24]. In this paper, we choose a single-chip DSP as the kernel in the implementation of a digital controller and adopt the software approach in the realization of the fuzzy-

tuning current-control algorithm. The fuzzy decision table was first off-line computed and then stored in an EPROM. Therefore, the tuning process is basically performed on a lookup table and can be executed very quickly.

Fig. 8 shows the hardware architecture of the DSP-based fuzzy-tuning current controller. The kernel of the FTC is

TABLE I  
PARAMETERS OF THE PWM INVERTER DRIVE UNDER TESTING

3-phase induction motor	
Type: 3-phase, Y-connection, 2-pole, 800W	
stator resistance	$R_s = 1.1\Omega$
stator inductance	$L_s = 0.145\text{H}$
mutual inductance	$L_m = 0.136\text{H}$
rotor resistance	$R_r = 1.3\Omega$
rotor inductance	$L_r = 0.145\text{H}$
PWM inverter	
dc link voltage	$V_{dc} = 150$ volts
rated current	$I_A = 10$ Amps
PWM switching frequency	5 kHz
digital control sampling frequency	5 kHz

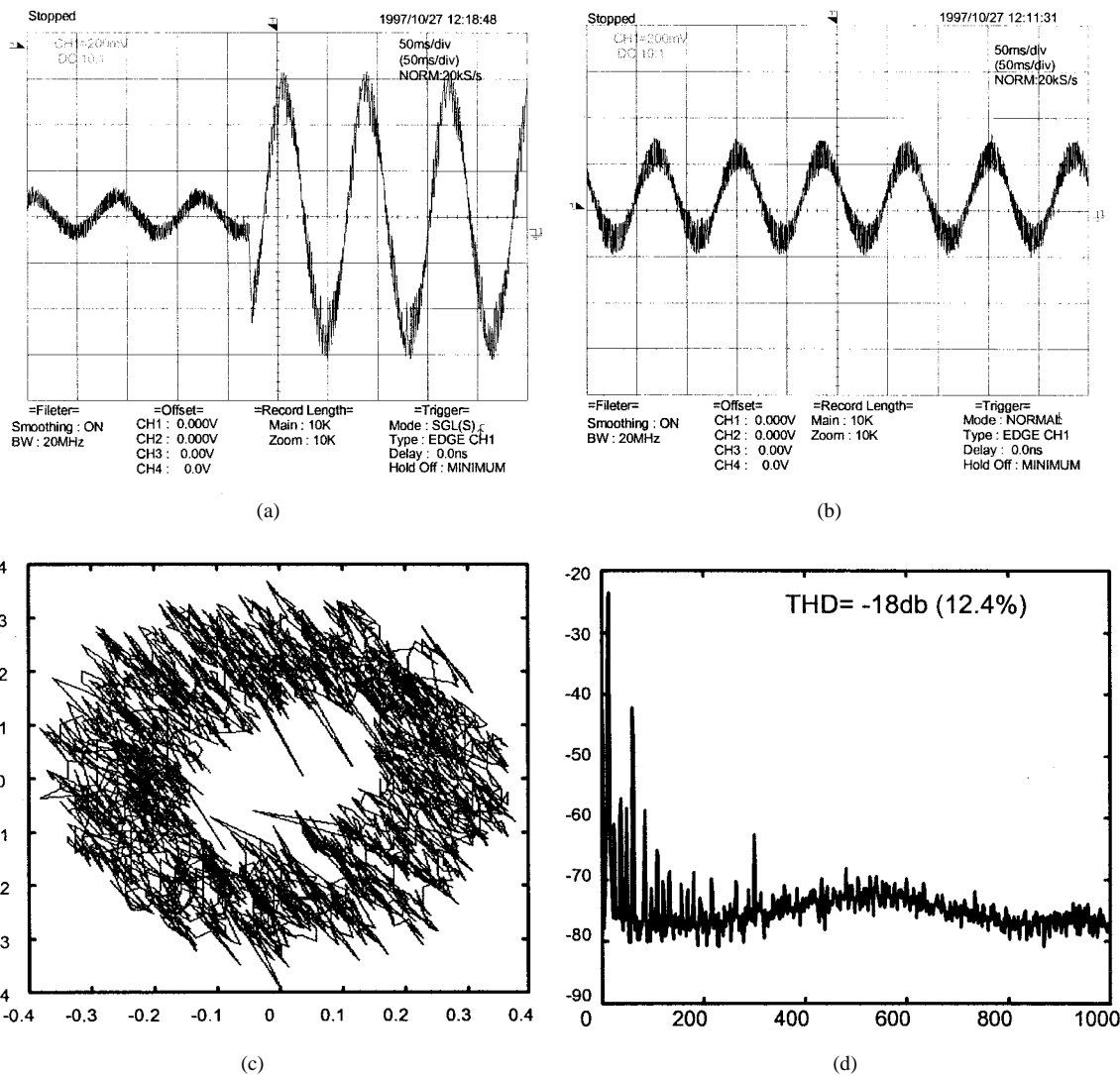


Fig. 9. Experimental results of the switched hysteresis current controller. (a) Step response. (b) Steady-state response of the phase current. (c) Current-vector trajectory in steady state. (d) Harmonics spectrum.

a single-chip DSP (TMS320C14) from Texas Instruments which is running at 25 MHz and has 256 words of on-

chip RAM and 4 K words of on-chip program ROM. Its instruction cycle is 200 ns and most of the instructions are one-

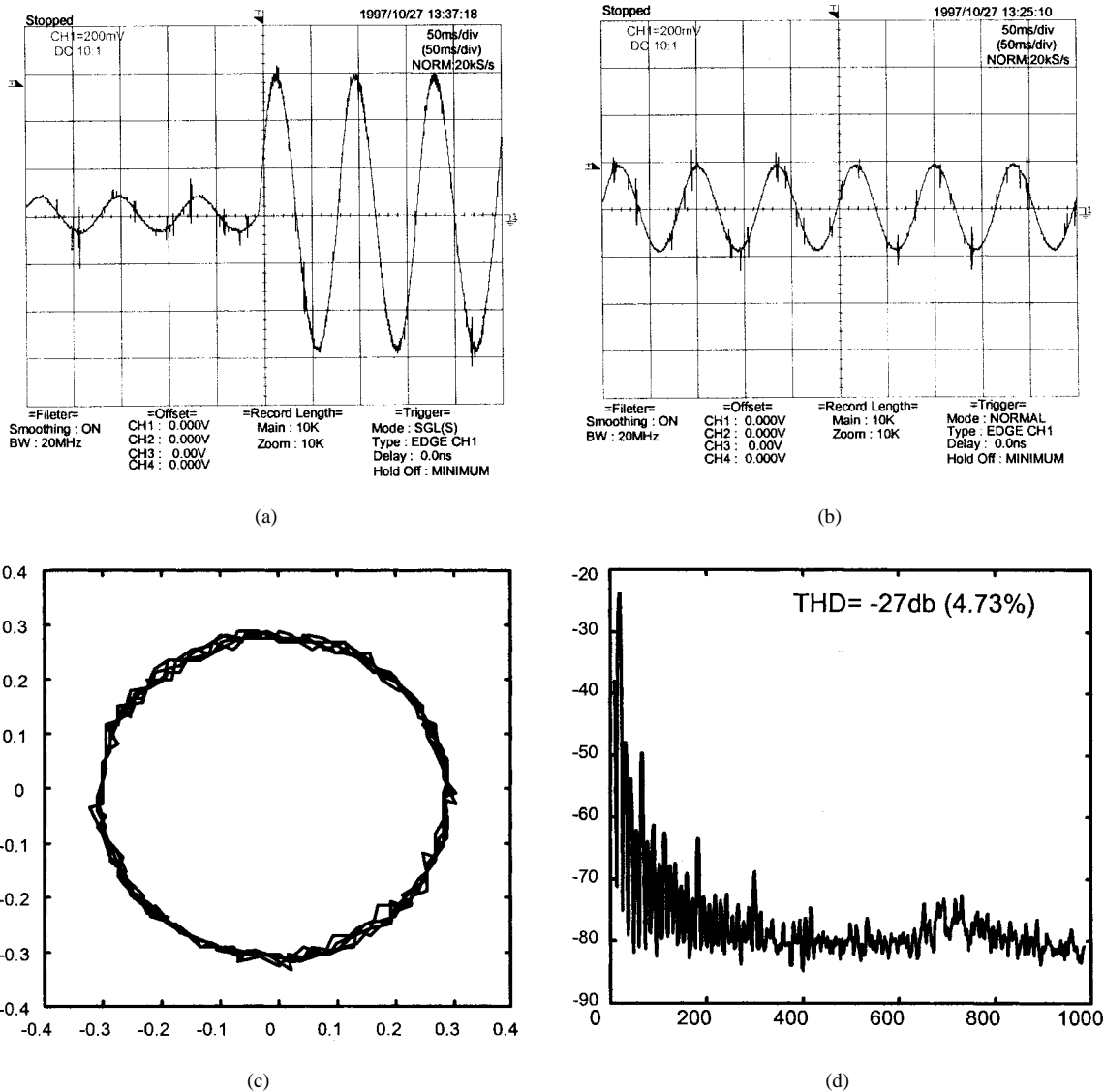


Fig. 10. Experimental results of the proposed FTC scheme: (a) step response and (b) steady-state response of the phase current, (c) current vector trajectory in steady state, and (d) harmonics spectrum.

cycle instructions. This DSP reaches a benchmark computation speed up to 8.77 million instructions per second (MIPS) [31]. The most attractive features of this DSP is its I/O handling capability. It has an event manager with four-capture input and six-compare output, a programmable I/O port, a serial port with programmable protocols and timers, a watchdog timer, and two general purpose programmable timers. The high computation speed and I/O functions of the TMS320C14 make it especially suitable in applications of power electronics and motion control.

Hysteresis current control of PWM inverters has been studied a great deal in the literature [5]–[9]. Hysteresis control schemes are usually realized using analog circuitry due to the requirement of instantaneous response. Analog realization of hysteresis control with fixed band provides a simple way for current control of PWM inverters. However, the software realization of a hysteresis comparator will raise engineering difficulties not economically feasible to overcome, such as

analog-to-digital conversion delay, computation delay, and task swapping delay caused by interrupts of other control loops. For the purpose of comparison, using the same realization technique, the proposed FTC control scheme is compared with a switched hysteresis controller. The switched hysteresis controller functions as a digital bang-bang controller with a specified comparison level. The switched hysteresis controller outputs a maximum actuating force if the feedback is lower than its comparison level, otherwise, it outputs a maximum inverse actuating force. The simplicity of the switched hysteresis controller makes it a good standard for comparison analysis.

For the purpose of comparison, we purposely lower the PWM switching and sampling frequency; they are both set at 5 kHz and the output modulation frequency is 12 Hz. The ratings of the PWM inverter and parameters of the motor under testing are listed in Table I. Fig. 9 shows the experimental results of a PWM inverter using the switched hysteresis control



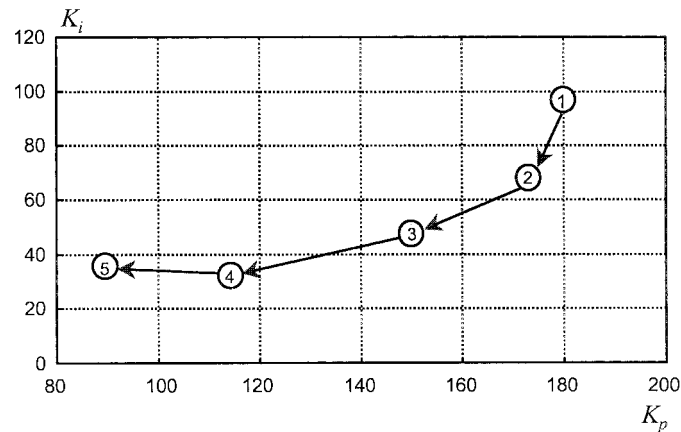


Fig. 11. Fuzzy-tuning trajectory of the control parameters of the PI controller.

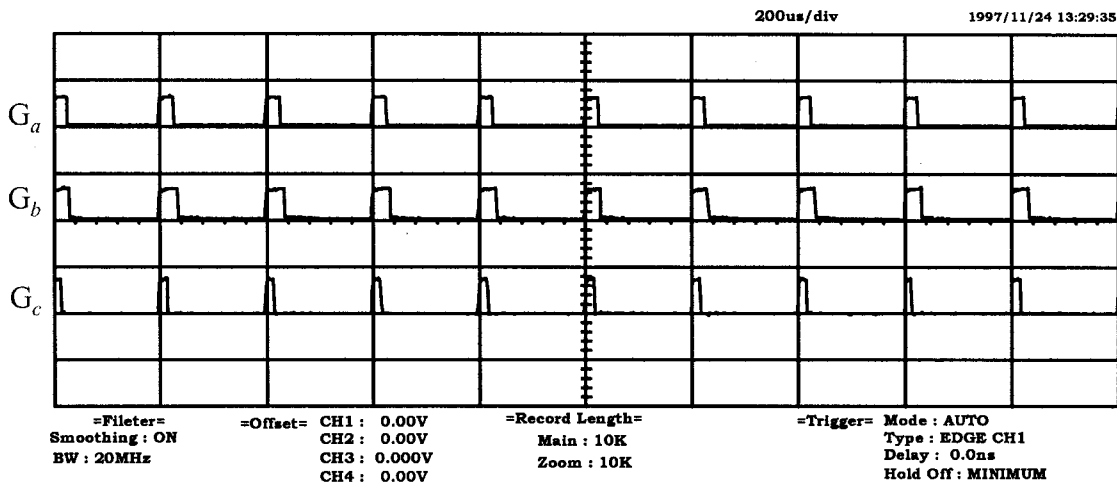


Fig. 12. Quasi-optimum PWM waveforms of the load current-vector trajectory after the self-tuning process.

scheme. Fig. 9(a) is the time response of phase current due to a step-changed sinusoidal command, Fig. 9(b) is the steady-state current response, Fig. 9(c) is the current-vector trajectory, and Fig. 9(d) is its corresponding frequency spectrum. Fig. 10 shows the experimental results of the proposed FTC-controlled PWM inverter under the same testing condition as in Fig. 9. Fig. 10(c) and Fig. 9(c) show the current trajectories of the two controllers on the  $dq$  plane. The length of the line segment represents the magnitude of the current-vector deviation. A longer line segment means a larger current ripple in its time response. It can be observed that larger current ripples resulted by using the conventional hysteresis current control scheme.

Fig. 11 records the fuzzy-tuning trajectory of the control parameters of the current-loop PI controller during its steady-state operation period. Fig. 12 shows the steady-state PWM gating signals for the PWM inverter after the fuzzy-tuning process. These quasi-optimum PWM signals can control the current-vector trajectory to follow its desired path without small random circles. If we compare Fig. 10(d) with Fig. 11(d),

we can observe that the proposed FTC scheme can significantly reduce the THD of the current waveforms. Experimental results show the self-tuning current controller can effectively reduce the PWM inverter current ripples in steady state and, at the same time, maintain a fast current transient response.

## V. CONCLUSION

In this paper, we have developed a new discrete FTC scheme for the current regulation of three-phase PWM inverters. The proposed current control scheme can achieve fast transient responses and, at the same time, have very low THD in output current during steady-state operation. The proposed FTC scheme generates quasi-optimum PWM patterns by using closed-loop control technique with instantaneous current feedback. Experimental results have shown that the proposed FTC scheme can achieve low current ripple at low switching frequency in steady state without knowing the motor parameters.

## REFERENCES

- [1] C. D. Schauder and R. Caddy, "Current control of voltage source inverters for fast four quadrant drive performance," *IEEE Trans. Ind. Applicat.*, vol. IA-18, pp. 163–171, Mar./Apr. 1982.
- [2] C. K. Taft and E. V. Slate, "Pulsewidth modulated DC motor control: A parameter variation study with current loop analysis," *IEEE Trans. Ind. Electron. Contr. Instrum.*, vol. IECI-26, pp. 218–226, Nov. 1979.
- [3] L. Malesani and P. Tomasin, "PWM current control techniques of voltage source converters—A survey," in *Conf. Rec. IEEE IECON*, 1993, pp. 670–675.
- [4] M. P. Kazmierkowski and M. A. Dzieniakowski, "Review of current control regulation techniques for 3-phase PWM inverters," in *Conf. Rec. IEEE IECON*, 1994, pp. 567–575.
- [5] A. B. Plunkett, "A current controlled PWM transistor inverted drive," in *Conf. Rec. IEEE-IAS Annu. Meeting*, 1979, pp. 785–792.
- [6] P. Enjeti, P. D. Ziogas, J. F. Lindsay, and M. H. Rashid, "A novel current controlled PWM inverter for variable speed ac drives," in *Conf. Rec. IEEE-IAS Annu. Meeting*, 1986, pp. 235–243.
- [7] D. M. Brod and D. W. Novotny, "Current control of VSI-PWM inverters," *IEEE Trans. Ind. Applicat.*, vol. IA-21, pp. 562–570, May/June 1985.
- [8] B. K. Bose, "An adaptive hysteresis-band current control technique of a voltage-fed PWM inverter for machine drive system," *IEEE Trans. Ind. Applicat.*, vol. 37, pp. 142–150, Sept./Oct. 1990.
- [9] A. Tripathi and P. C. Sen, "Comparative analysis of fixed and sinusoidal band hysteresis current controllers for voltage source inverters," *IEEE Trans. Ind. Electron.*, vol. 39, pp. 63–73, Feb. 1992.
- [10] H. W. van der Broeck, H. C. Skudelny, and G. V. Stanke, "Analysis and realization of a pulsewidth modulator based on voltage space vectors," *IEEE Trans. Ind. Applicat.*, vol. 24, pp. 142–150, Jan./Feb. 1988.
- [11] M. Morimoto, S. Sato, K. Sumito, and K. Oshitani, "Single-chip microcomputer control of the inverter by the magnetic flux control PWM method," *IEEE Trans. Ind. Electron.*, vol. 36, pp. 42–47, Feb. 1989.
- [12] S. Fukuda, Y. Iwaji, and H. Hasegawa, "PWM technique for inverter with sinusoidal output current," *IEEE Trans. Power Electron.*, vol. 5, pp. 54–61, Jan. 1990.
- [13] A. Nabae, S. Ogasawara, and H. Akagi, "A novel control scheme for current-controlled PWM inverters," *IEEE Trans. Ind. Applicat.*, vol. IA-22, pp. 697–701, July/Aug. 1986.
- [14] I. Miki, O. Nakao, and S. Nishiyama, "A new simplified current control method for field oriented induction motor drives," in *Conf. Rec. IEEE-IAS Annu. Meeting*, 1989, pp. 390–395.
- [15] T. G. Habetler and D. M. Divan, "Performance characterization of a new discrete pulse-modulated current regulator," *IEEE Trans. Ind. Applicat.*, vol. 25, pp. 1139–1148, Nov./Dec. 1989.
- [16] M. P. Kazmierkowski, M. A. Dzieniakowski, and W. Sulkowski, "Novel space vector based current controllers for PWM-inverters," *IEEE Trans. Power Electron.*, vol. 6, pp. 158–165, Jan. 1991.
- [17] D. S. Oh, K. Y. Cho, and M. J. Youn, "A discretized current control technique with delayed input voltage feedback for a voltage-fed PWM inverter," *IEEE Trans. Power Electron.*, vol. 7, pp. 364–373, Apr. 1992.
- [18] S. K. Sul, B. H. Kwon, J. K. Kang, K. Y. Lim, and M. H. Park, "Design of an optimal discrete current regulator," in *Conf. Rec. IEEE-IAS Annu. Meeting*, 1989, pp. 350–354.
- [19] S. S. Min, K. C. Lee, J. W. Song, and K. B. Cho, "A fuzzy current controller for field-oriented controlled induction machine by fuzzy rule," in *Conf. Rec. IEEE PESC*, 1992, pp. 265–270.
- [20] L. A. Zadeh, "Fuzzy sets," *Inform. Contr.*, vol. 8, no. 6, pp. 338–353, June 1965.
- [21] E. H. Mamdani, "Application of fuzzy algorithms for control of a simple dynamic plant," *Proc. IEEE*, vol. 121, pp. 1585–1588, Dec. 1974.
- [22] R. J. Marks II, Ed., *Fuzzy Logic Technology and Applications*. Piscataway, NJ: IEEE Press, 1994.
- [23] M. Jamshidi, N. Vadiiee, and T. Ross, *Fuzzy Logic and Control: Software and Hardware Applications*. Englewood Cliffs, NJ: Prentice-Hall, 1993.
- [24] C. C. Lee, "Fuzzy logic in control systems: fuzzy logic controller—Part I, II," *IEEE Trans. Syst., Man, Cybern.*, vol. 20, pp. 404–435, Mar./Apr. 1990.
- [25] F. V. D. Rhee, H. R. V. N. Lemke, and J. G. Dijkman, "Knowledge based fuzzy control of systems," *IEEE Trans. Automat. Contr.*, vol. 35, pp. 148–155, Feb. 1990.
- [26] L. X. Wang and J. M. Mendel, "Generating fuzzy rules by learning from examples," *IEEE Trans. Syst., Man, Cybern.*, vol. 22, pp. 1414–1427, Nov./Dec. 1992.
- [27] H. Ishibuchi, K. Nozaki, and H. Tanaka, "Empirical study on learning in fuzzy systems," in *Proc. IEEE Int. Conf. Fuzzy Systems*, 1993, pp. 606–611.
- [28] H. T. Nguyen, V. Kreinovich, and D. Tolbert, "On robustness of fuzzy logics," in *Proc. IEEE Int. Conf. Fuzzy Systems*, 1993, pp. 543–547.
- [29] H. T. Nguyen, C. W. Tao, and W. E. Thompson, "An empirical study of robustness of fuzzy systems," in *Proc. IEEE Int. Conf. Fuzzy Systems*, 1993, pp. 1340–1345.
- [30] H. J. Zimmerman, *Fuzzy Set Theory and its Applications*. Amsterdam, The Netherlands: Kluwer, 1991.
- [31] *TMS320C1x User's Guide*, Texas Instruments, Incorporated, Dallas, TX, July 1991.



**Ying-Yu Tzou** (S'82–M'88) was born in Taiwan, R.O.C., in 1956. He received the B.S. and M.S. degrees in control engineering from National Chiao Tung University, Hsinchu, Taiwan, R.O.C., and the Ph.D. degree in electrical engineering from the Institute of Electronics Engineering, National Chiao Tung University, in 1978, 1983, and 1987, respectively.

During 1980–1981, he was with the Electronic Research and Service Organization (ERSO) of the Industry Technology Research Institute (ITRI) as a Design Engineer in the Control System Department. During 1983–1986, he was a Project Manager with Microtek Automation, Inc., involved in the development of a computer numerical controller (CNC) for machine tools. He is currently a Professor in the Department of Electrical and Control Engineering, National Chiao Tung University, and also serves as an Industrial Consultant for many local power electronics and automation companies. He was the Director of the Institute of Control Engineering during 1992–1994. His special interests are currently sensorless ac drives, intelligent UPS, FPGA-based control IC's for motor drives and power converters, and DSP applications in power electronics and motion control.



**Shiu-Yung Lin** was born in Taipei, Taiwan, R.O.C., in 1971. He received the M.S. degree in 1997 from National Chiao Tung University, Hsinchu, Taiwan, R.O.C., where he is currently working towards the Ph.D. degree in the Department of Electrical and Control Engineering.

His research interests are in the areas of power electronics and motion control. His current research involves DSP-based induction motor sensorless control, self-tuning control, and self-commissioning control.